Project A: Fuel Cell

Name of Student:
Le Hoang Khang - 98083

Mentor:
Prof./Dr. Pinkward Karten
Margarita Aleksandrova

10.30. – 11.20.2024

Contents

1 Introduction

With the rapid growth of electric vehicles, there is a global shift towards clean and sustainable energy sources to power them. Among these, fuel cells have emerged as a promising technology. Fuel cells are not only adaptable to various energy system requirements, but they are also well-suited for electric vehicles due to their high-power density. A key advantage that sets fuel cells apart from traditional energy sources is their clean output. Unlike conventional fuels like gasoline, fuel cells produce only water, heat, and electricity as by-products, making them an environmentally friendly solution that can contribute significantly to reducing global pollution [1]. This project aims to explore, understand, and experiment with fuel cell technology in the lab at Karlsruhe University of Applied Sciences. Through hands-on research, the characteristics and performance of fuel cells will be examined, with a particular focus on the behavior of a 10-year-old fuel cell. This study will provide valuable insights into the long-term efficiency and sustainability of fuel cells as a viable power source for the future.

2 Theoritical part

2.1 Overview fuel Cell

A fuel cell is an electrochemical device that converts energy from various fuels—such as hydrogen - directly into electricity, using an oxidant like oxygen from the air. As shown in Figure 1, a fuel cell consists of an electrolyte layer positioned between two electrodes. It operates similarly to a battery, relying on a redox reaction, which is separated into independent anodic oxidation and cathodic reduction processes [2].
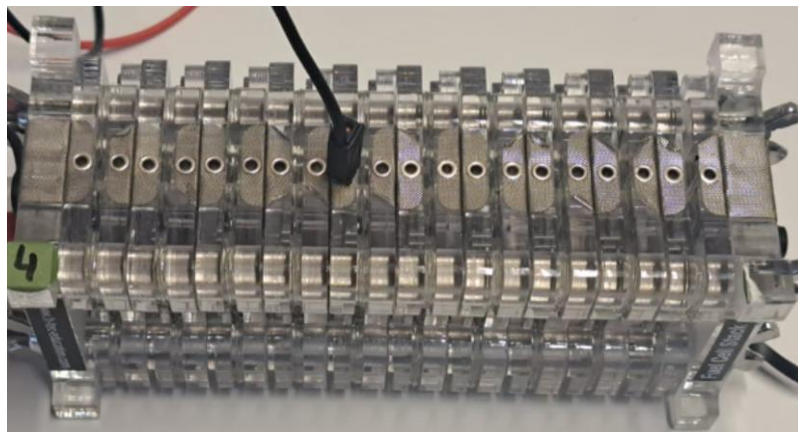

Figure 1 . Hydrogen fuel cell in Power Lab in Karlsruhe University of Applied Science.

The specific fuel used in a fuel cell can vary depending on the type, but all fuel cells are fundamentally based on redox (reduction-oxidation) reactions. At the anode, the fuel undergoes oxidation, releasing electrons and ions. While ions move through the electrolyte or membrane separating the two electrodes, the electrons are blocked and diverted through an external circuit to the cathode, generating an electric current. This process is efficient and produces minimal
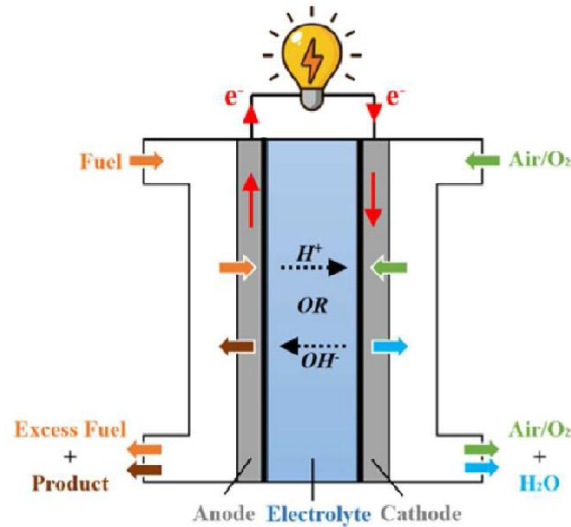
emissions, with water and heat as the primary by-products [1,3].

Figure 2 General working principle of conventional rigid fuel cell [2].

2.1.1 Performance of the fuel cell

The performance of a fuel cell can be evaluated based on several key factors: energy density, lifetime, and application suitability. Fuel cells offer a very high energy density, allowing them to provide sustained power over extended periods. One notable feature of fuel cells is the separation between the fuel tank and the electrodes. This design characteristic enhances application flexibility, as varying the capacity and quantity of electrodes within the fuel cell allows for a broad range of power and capacity outputs. According to research by M.A. Aminudin [2], fuel cells exhibit higher efficiency and power density compared to traditional batteries, as illustrated in Figure 2 and Table 1. Additionally, there is a significant difference in the 2019 shipment volumes of hydrogen fuel cells and lithium-ion batteries, with hydrogen fuel cells far surpassing fuel cells in market adoption for that year.
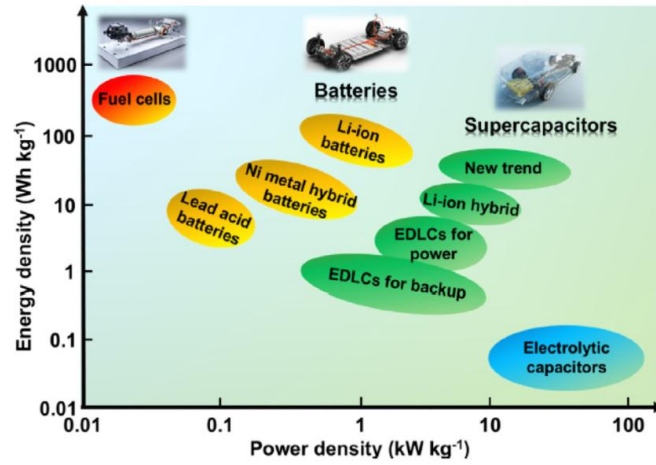
Figure 3 Ragone plot of several new energy technologies [2].

Table 1 Characteristic of fuel cell and lithium-ion battery [2].

Charge Carrier	Operating Temperature	Electrical Efficiency	Primary Fuel	Shipments in 2019
PEMFCs	-40 to 120 °C (150-180 °C in high temp PEMFCs)	Up to 65-72%	H_2, reformed H_2, methanol in direct methanol fuel cells	934.2 MW
AFCs	50-200 °C	Up to 70%	H_2 or cracked ammonia	0 MW
PAFCs	150-220 °C	Up to 45%	H_2 or reformed H_2	106.7 MW
MCFCs	600-700 °C	Up to 60%	H_2, biogas, or methane	10.2 MW
SOFCs	500-1000 °C	Up to 65%	H_2, biogas, or methane	78.1 MW
Lithium Battery	15-60 °C	Up to 90%	Lithium-ion	400 MW

There are various types of fuel cells, but for this case, based on [1], the types considered are MCFC, SOFC, HPEFC, AFC, PAFC, PEMFC, and DMFC. These fuel cells can be categorized into three groups based on their operating temperatures. For high and medium-temperature applications, MCFC, SOFC, and HPEFC operate at temperatures above 120°C. In contrast, for low-temperature applications, AFC, PEMFC, and PAFC function at temperatures below 120°C. There are also more characteristic to distinguish the fuel cells such as the Aggregate stage electrolyte, pH value of the electrolyte, direct fuel cell or reformer type fuel cell. But for this project, the diversion based on the working temperature is used for easy separation purpose.

.

2.1.2 Elements of a generic bipolar fuel cell

A generic bipolar fuel cell is consisting of several elements as Figure 5 that enable the efficiency on power generation. The main components of it are bipolar plates in Figure 4, which connect individual cells in series to form a stack, which increase the output power. These plates conduct electricity, distribute fuel and oxidant, and manage the removal of heat and water by-products [4].

Figure 4. A metallic fuel cell bipolar plate of Cell form [4].

Within each cell, the anode and cathode electrodes facilitate the redox reactions—where fuel oxidizes at the anode and the oxidant reduces at the cathode. Between these electrodes lies the electrolyte or membrane, which allows ions to pass while forcing electrons through an external circuit to generate current. This modular, compact structure makes bipolar fuel cells adaptable for high-power applications, with the ability to add more cells to meet various power requirements. Additionally, the gas diffusion layer (GDL) ensures even distribution of gases and aids in water management, while end plates stabilize the entire stack.
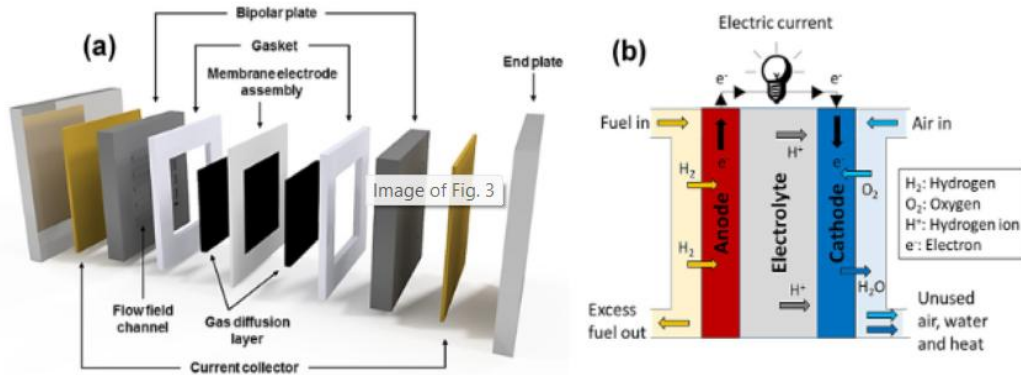
Figure 5. (a) Polymer electrolyte membrane fuel cell (PEMFC) main components and (b) the membrane electrode assembly schematic diagram (MEA) [2].

2.1.3 Advantages and disadvantages of the fuel cell

Fuel cells (FCs) offer various advantages, but two of their most notable characteristics are their high-power density and adaptability. The first advantage is the power density of fuel cells. According to [1,3], the general power density of fuel cells is approximately 1200 Wh/kg, which

6

is four times higher than that of traditional batteries and forty times higher than that of supercapacitors. This high-power density makes fuel cells highly efficient for energy-demanding applications. Another significant advantage of fuel cells is their adaptability to different power systems, from mobile applications to standby power systems. This adap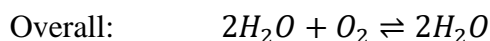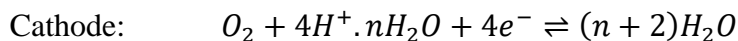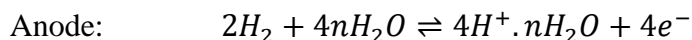tability is due to the structure of fuel cells, where the fuel tank and electrodes are separate. If capacity is a priority, the fuel cell system can be adjusted by increasing the size of the fuel tank. Conversely, if high power output is needed, the system can incorporate additional electrodes or cells to enhance performance.

As a result, fuel cells have been researched and developed to meet a wide range of requirements across numerous power systems. However, a major drawback of fuel cells is their high cost, particularly when applied on a larger scale. Fuel cells are expensive due to the cost of producing hydrogen fuel. Additionally, producing green hydrogen through electrolysis requires rare metals like iridium and platinum, which further drive-up costs [4]. This expense remains a significant barrier to widespread fuel cell adoption.

2.2 PEM Fuel Cell

The proton exchange membrane fuel cell (PEMFC) shares a similar structure with other fuel cells but is distinguished by its polymer electrolyte membrane, a critical component that facilitates proton conductivity. In the core chemical process, hydrogen at the anode splits into protons and electrons.

Anode: $2H_2 + 4nH_2O \rightleftharpoons 4H^+.nH_2O + 4e^-$

Cathode: $O_2 + 4H^+.nH_2O + 4e^- \rightleftharpoons (n+2)H_2O$

Overall: $2H_2O + O_2 \rightleftharpoons 2H_2O$

The protons pass through the membrane to the cathode, while the electrons travel through an external circuit, generating electrical power. At the cathode, protons, electrons, and oxygen combine to form water as a by-product. Operating within a relatively low temperature range, typically between -40°C and 120°C, PEMFCs are noted for their high-power density, making them well-suited for applications in transportation and portable power. Despite these advantages, PEMFCs face limitations, including the high cost of platinum catalysts, the durability of the membrane, and the challenges associated with hydrogen storage. These factors currently restrict their widespread use, though PEMFCs remain a promising technology for clean energy generation.
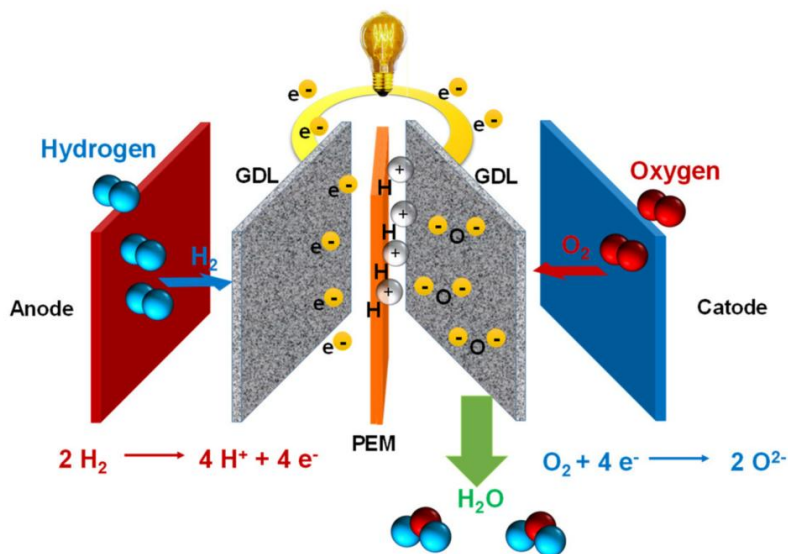
Figure 6. Schematic diagram showing the components of a single PEMFC: anode, cathode, gas diffusion layer (GDL), membrane, anode, and cathode reactions together and products [6].

2.3 Hydrogen

Hydrogen plays a crucial role as the fuel source for proton exchange membrane fuel cells (PEMFCs). It can be produced from a variety of sources, including fossil fuels like oil and natural gas, renewable resources such as biomass, or through water splitting using solar or electrical energy. The two most common methods for hydrogen production are steam-methane reforming and electrolysis. Steam-methane reforming, which uses high-temperature steam to

react with methane under pressure in the presence of a catalyst, is widely used in the United States, accounting for the majority of commercially produced hydrogen. However, this process releases carbon monoxide and carbon dioxide as by-products. Electrolysis, on the other hand, produces hydrogen by splitting water with electricity, achieving an efficiency of approximately 60-80%, especially when renewable energy sources are used.

After hydrogen is produced, it can be stored through various methods, categorized into two primary types: physical-based and material-based. Physical-based storage includes options like compressed gas, cryo-compressed storage, and liquid hydrogen, where hydrogen is stored in gaseous or liquid form to optimize density. Material-based storage involves storing hydrogen within materials, such as adsorbents, liquid organics, and different types of hydrides. Each storage method has specific characteristics that make it suitable for different applications, balancing factors such as storage density, temperature requirements, and energy efficiency.
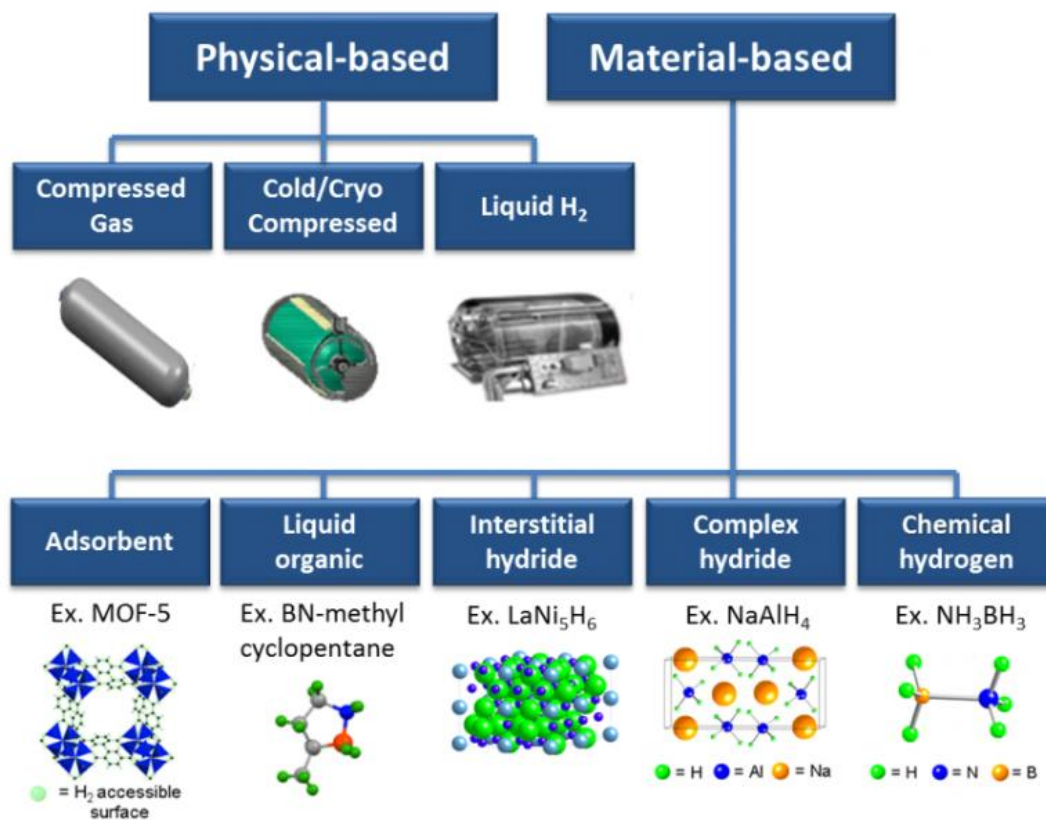
Figure 7. Ways to store Hydrogen [10].

3 Experiment

3.1 Characteristic curve of hydrogen Fuel Cell

3.1.1 Description of experiment

The primary goal of the first experiment is to build a characteristic curve of a hydrogen PEMFC. The components used in this experiment are shown in Figure 8. Four cells from the lab's fuel cell system are utilized to examine the fuel cell's characteristic curve. To collect and store data on voltage, current, and power, a measurement device and a computer are connected to the fuel cell system. A hydrogen generator, powered by a 4.5V supply, serves as the fuel source. This generator separates hydrogen from water, supplying hydrogen directly to the fuel cell system. Once the hydrogen is supplied, the measurement device simulates the load and captures data to generate the characteristic curve. The collected data is displayed on the computer and stored in a text format for further analysis. Noted that in the app on the computer lab, the mode "Automatic" is chose.
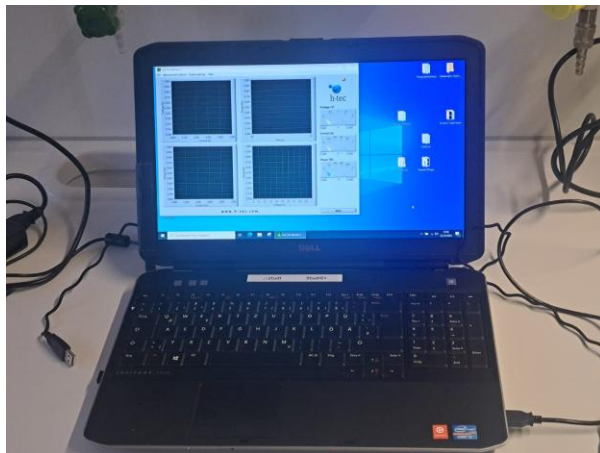
a)   Lab computer
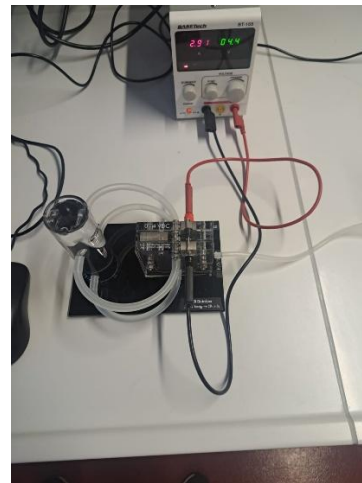
b)   Hydrogen fuel generator
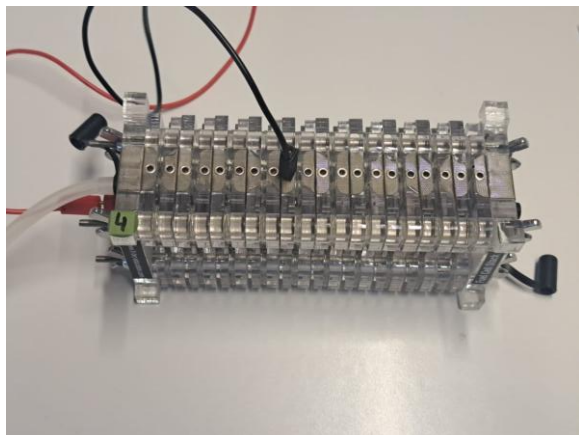
c) Fuel cell
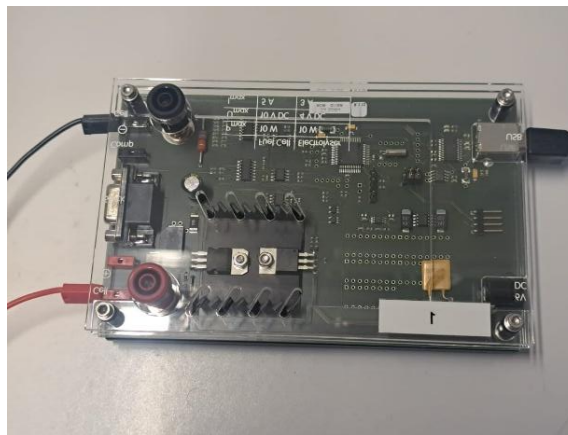
d) Measurement device

Figure 8. Experiment devices.
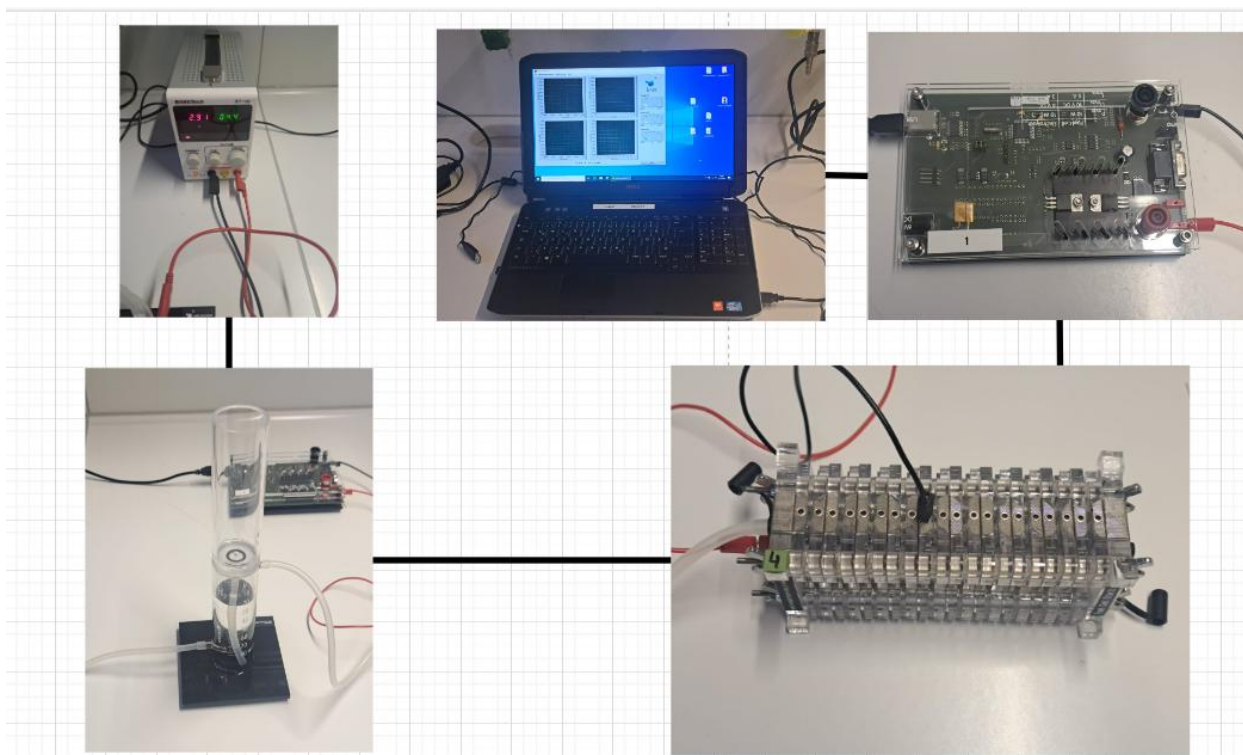
Figure 9. The experiment set up

3.1.2 Results – diagram, table, graphics

The result of the experiment is showed in figure 10 and 11. The characteristic curve is recorded 2nd times and plotted into power – current graph and voltage-current graph.
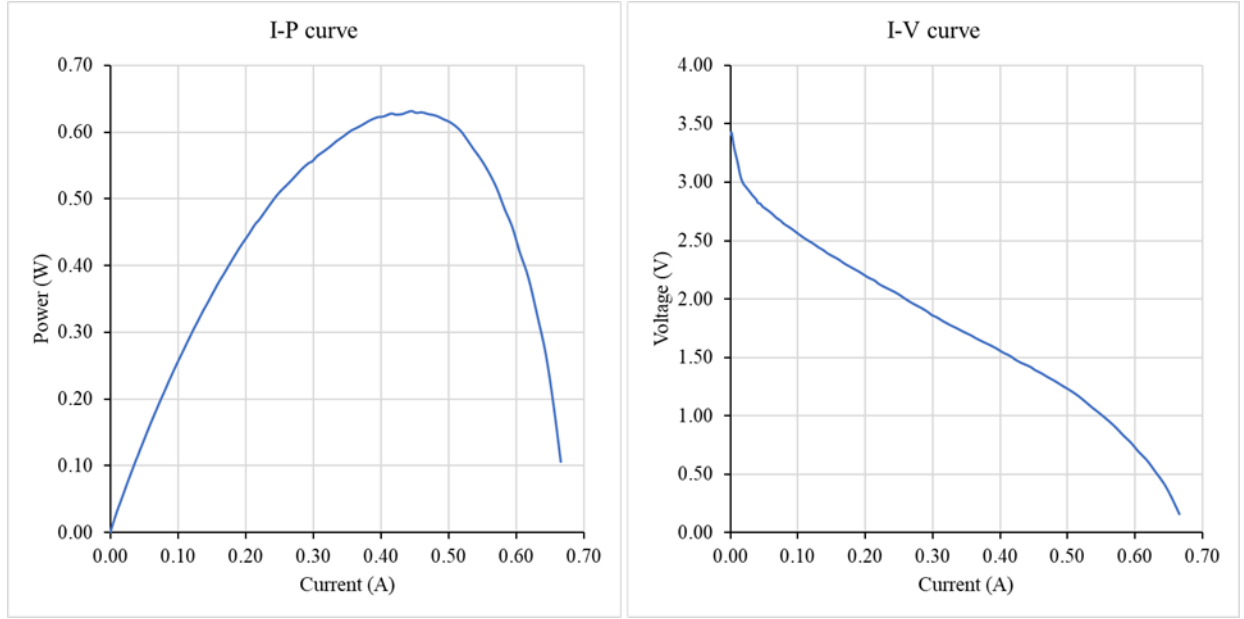
a)
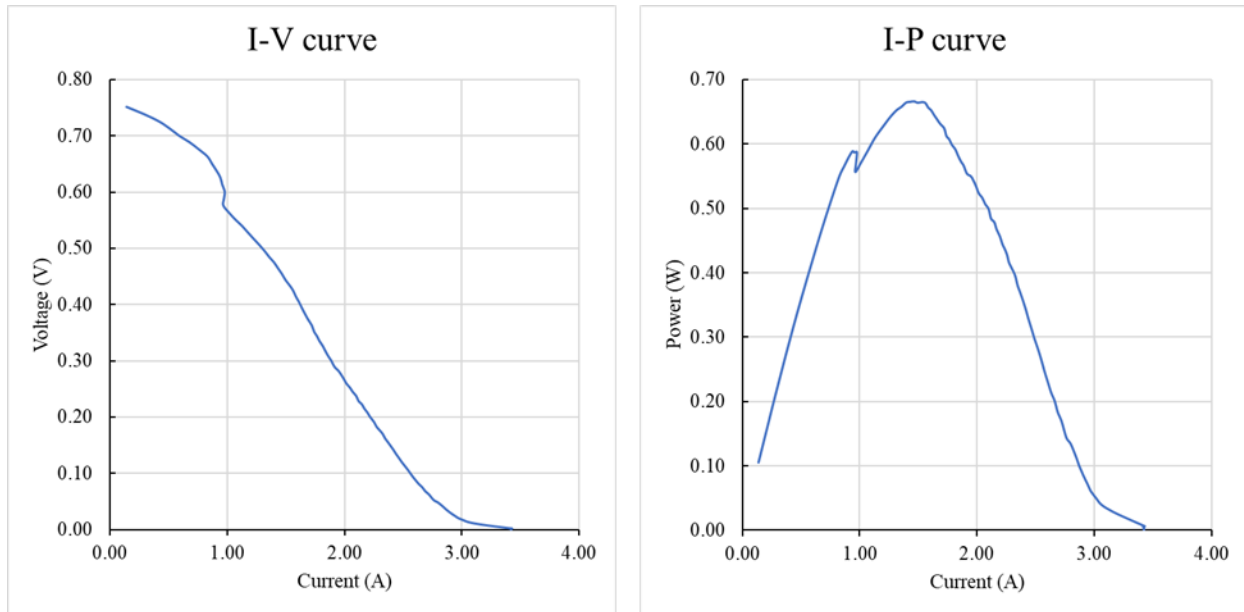
b)

Figure 10.a) The first record of the I-V and I-P characteristic curve, b) The second record of the I-V and I-P characteristic curve

3.1.3 Discussion of results

This figure illustrates the first recorded I-V and I-P characteristic curves of a hydrogen PEMFC system. The I-V curve (left) shows the relationship between the current (A) and voltage (V), highlighting the voltage drop as current increases due to internal resistance and fuel cell polarization. The characteristic of a FC system has 3 phases, which is corresponded to theoretical phased in [12].

a).
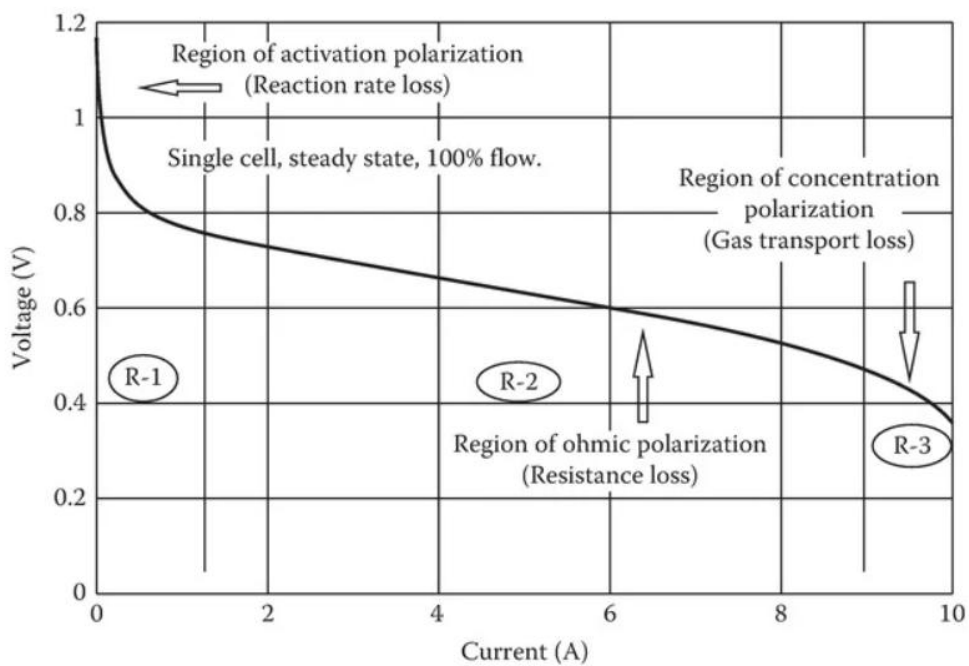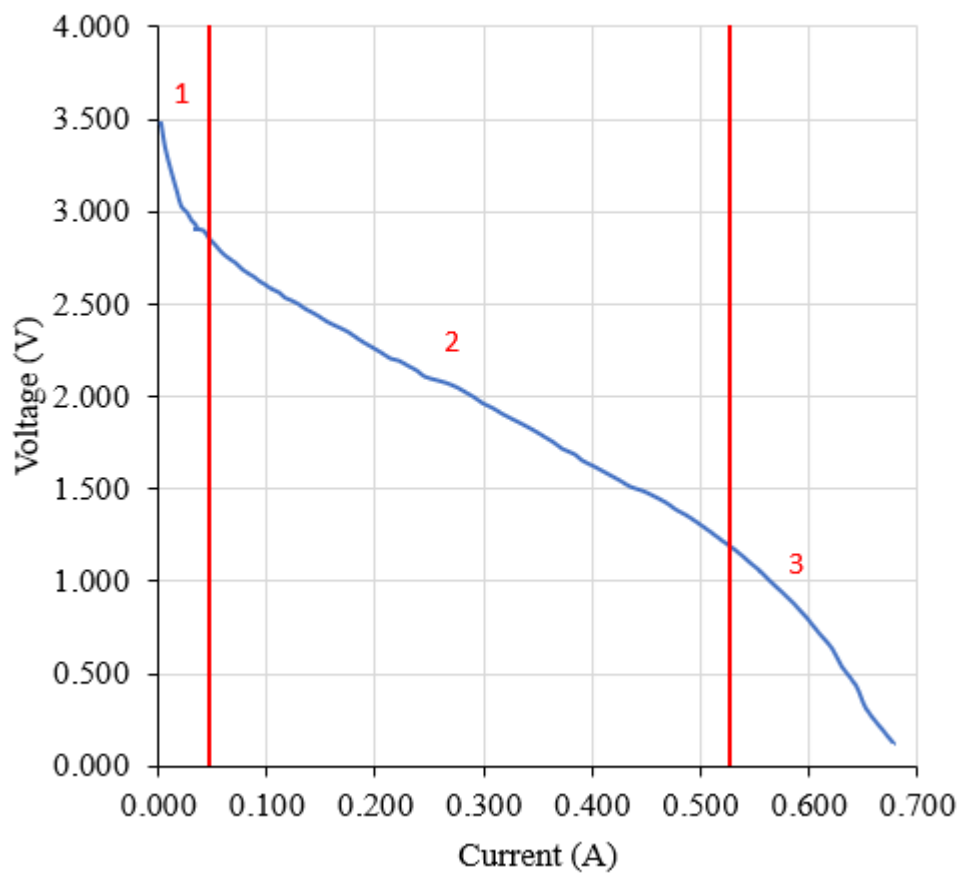
b).

Figure 11. a) Typical fuel cell V–I characteristic curve [13] b) Region in recorded characteristic curve.

The first region, ranging between 0–0.5 A, represents the activation losses, as shown in region 1 of Figure 11.b). In this region, a steep voltage drop is observed due to the energy required to overcome the electrochemical reaction barriers at the electrodes. These losses are primarily caused by the sluggish kinetics of reactions, particularly the oxygen reduction reaction at the cathode. A critical factor influencing this region is the exchange current density (i_0), a key electrochemical parameter that represents the rate of electron exchange at an electrode's surface under equilibrium conditions, where no net current flows. A higher i_0 indicates faster and more efficient reactions, such as hydrogen oxidation at the anode and oxygen reduction at the cathode, reducing the energy required to initiate the reactions and minimizing the voltage drop. Catalysts, like platinum, are commonly used to increase i_0 and enhance reaction rates, although they contribute significantly to the fuel cell's cost. Therefore, i_0 is essential for reducing activation losses and improving the overall performance of the fuel cell in the activation region of the I-V curve.

The second region indicates on the Figure 11.b) is ohmic losses region. This region is ranged from 0.5 to 5.25 A. In this region, the voltage drop is almost linear. The cause of voltage loss is mostly from the electrical resistance of the electrodes, and the resistance to the flow of ions in the electrolyte. The size of the voltage drop is simply proportional to the current:

$$V = IR$$

Where V is voltage (V) of the FC, I is the current (A) of the FC and R is the total resistance (Ω) inside the FC.

Methods to reduce internal resistance include using highly conductive electrodes, optimizing the design and materials of bipolar plates, and minimizing electrolyte thickness while ensuring physical robustness and avoiding short circuits. These measures enhance overall fuel cell efficiency by addressing ohmic losses.

The final area is fuel cell mass transport losses, also known as concentration overvoltage, which are brought on by a decrease in reactant gas pressure or partial pressure while the cell is operating. During the process, oxygen is consumed at the cathode, which results in a minor decrease in its concentration. Likewise, flow resistance in supply ducts causes a pressure drop at the anode as a result of hydrogen consumption [12]. These losses are made worse by issues with PEMFCs including water removal and nitrogen accumulation, which obstructs the oxygen supply. This highlights how crucial effective reactant management is to fuel cell design.

In the second recorded result, a phenomenon resembling concentration overvoltage is observed, but it occurs at the start of the ohmic region. This drop is attributed as one of the four cells being filled with liquid water, a by-product of the fuel cell reaction. The accumulation of water blocks the air, hydrogen, and oxygen from reaching the proton exchange membrane (PEM), rendering that particular cell inactive. As a result, the blocked cell causes a voltage drop

within the ohmic region, highlighting the importance of effective water management to maintain consistent performance in fuel cell systems.

The I-P curve (right) depicts the power output (W) as a function of current, showing the peak power point where the fuel cell operates most efficiently before declining as current continues to rise. These curves provide essential insights into the fuel cell's performance, efficiency, and operational characteristics. The operating point, of the FC system are 1,427 V – 0,468A and 1,454V – 0,431A for the first and second record respectively.

In conclusion, the results clearly highlight the three main regions of the fuel cell's characteristic curve: activation losses, ohmic losses, and mass transport losses. Furthermore, a unique phenomenon was identified, resulting from the malfunctioning of a single cell in the fuel cell system due to water accumulation, which impeded performance. The analysis also reveals the operating point of the system, indicating the most balanced and stable power output that the fuel cell system can maintain.

3.2 Voltage controled measurements

3.2.1 Description of experiment

This experiment aims to maintain the voltage – load at a consistent value, therefore, the data of current and power over time are collected. Throughout the data, the approximate voltage for a stable power is obtained. In this case, voltage of load is decrease from 3.1 to 0.825 with 0.725 step. This experiment utilized the same set up in the previous experiment. However, in the app in computer lab, the mode is switched to "voltage controlled" mode and the constant voltage value is chosen.

3.2.2 Results – diagram, table, graphics

The result of the measurement is presented in Figure 12.
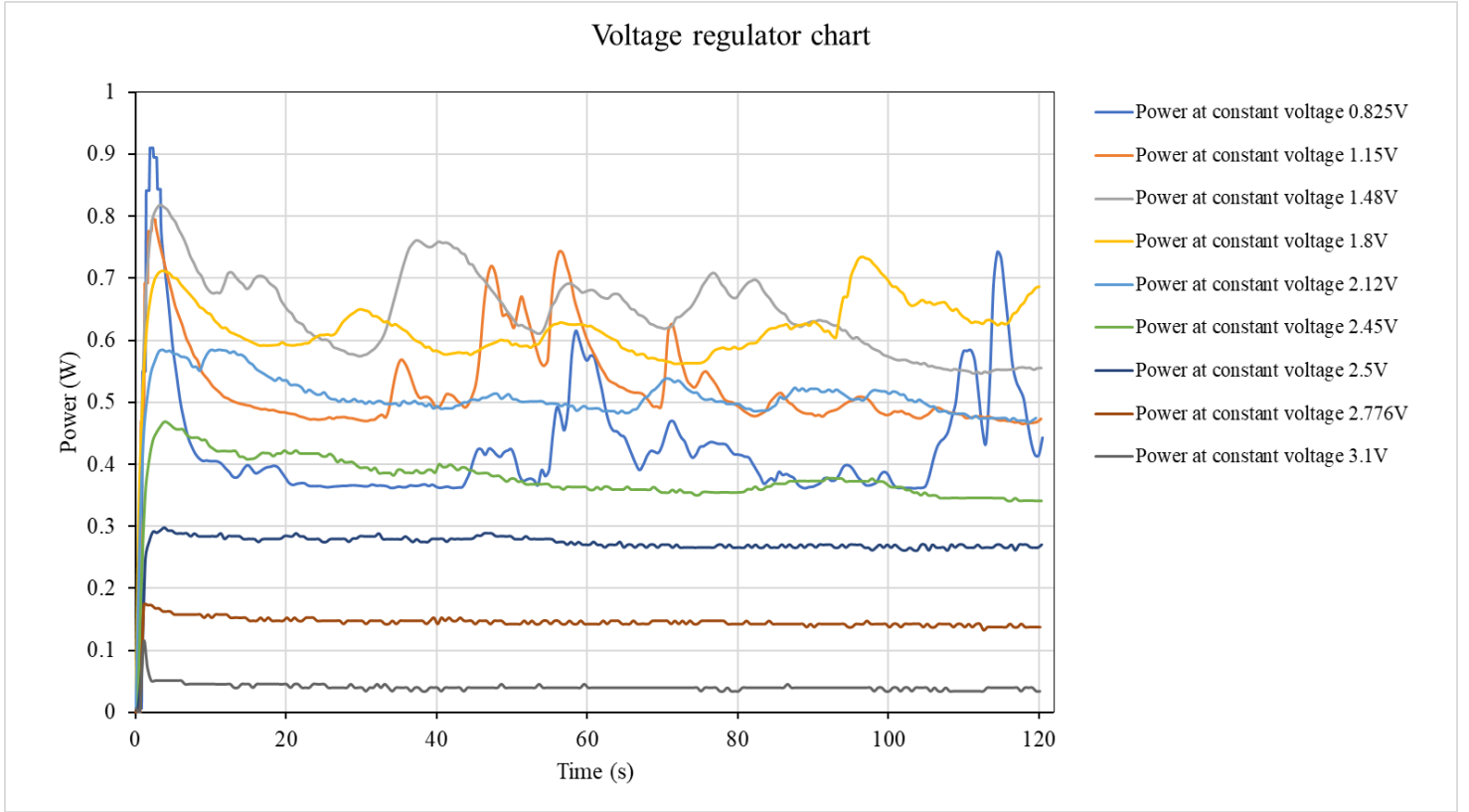
Figure 12. Power graph with different voltage regulator.

Table 2. Voltage-regulated characteristic curve of a fuel cell

No. of experiment	Voltage, V	Duration, sec	Sampling rate	Current, A	Power,W	Power stable
1	3,1	120	0.5	0,029	0,028	No
2	2,775	120	0.5	0,039	0,107	Yes
3	2,45	120	0.5	0,109	0,256	Yes
4	2,125	120	0.5	0,206	0,420	Yes
5	1,8	120	0.5	0,321	0,560	Yes
6	1,475	120	0.5	0,448	0,600	No
7	1,15	120	0.5	0,548	0,685	No
8	0,825	120	0.5	0,606	0,771	No
9	2,5	120	0.5	0,118	0,288	Yes

3.2.3 Discussion of results

Figure 12 illustrates the power output (in watts) over time (in seconds) for a fuel cell system operating at various constant voltage levels, ranging from 0.825V to 3.1V. The results indicate that voltages closer to the initial output of Ohmic region of the fuel cell achieve a more stable power output, as shown in table 2. Among these, the voltage range between 1.8V and 2.776V demonstrates higher stability, aligning with the ohmic region of the fuel cell's characteristic curve, where voltage decreases linearly with increasing current. Notably, the most

16

stable voltage observed in this experiment is 2.5V, suggesting it is an optimal operating point for steady performance in this system. The first peak every voltage regulator meet is due to the extra energy required to initial start the electrochemical reaction in the PEM. The reason of the fluctuating of the power when the voltage is maintained outside the Ohmic region, is the large voltage inside those regions.

3.3 Determination of efficiency

3.3.1 Description of experiment

This experiment aims to measure the volume of hydrogen produced over time and use the collected data, along with data from Experiment 1, to calculate the efficiency and energy efficiency of the fuel cell system. The experiment utilizes a hydrogen generator, starting with the system at an initial state where the water level in the upper section of the lab pipe is at zero. Upon turning on the power supply, hydrogen produced through the reverse reaction in the PEM pushes the water from the lower to the upper part of the pipe. The time taken for the water level to reach specific markers (e.g., 0, 5, 10, ..., 65 cm³) is recorded, representing the theoretical hydrogen volume. Then this data will be used to compare and calculate the efficiency and energetical efficiency of the fuel cell system.

3.3.2 Results – diagram, table, graphics

Figure 13 shows the linear increase of the hydro volume over time.
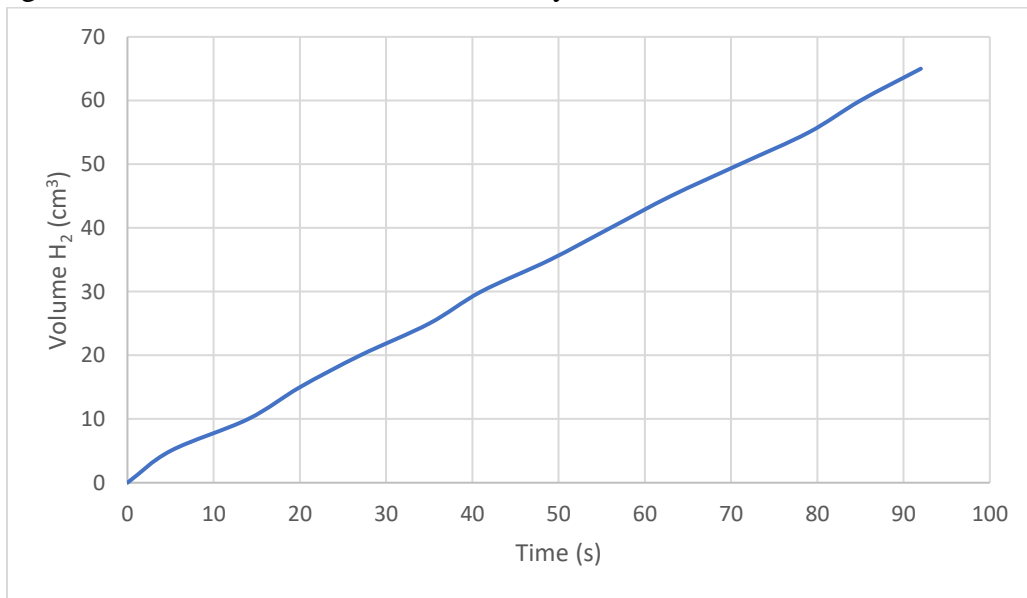
Figure 13. The theoretical produced hydrogen over time.

Table 3. Faraday efficiency (%) over time.

Time [s]	Voltage [V]	Current [A]	V_H2_exper (cm3)
0.31	3.41	0.00	0.21

17

0.81	3.42	0.00	0.56
1.31	3.42	0.00	0.91
1.81	3.42	0.00	1.25
2.31	3.43	0.00	1.60
2.81	3.43	0.00	1.95
3.31	3.28	0.01	2.30
3.81	3.15	0.01	2.64
4.31	3.06	0.01	2.99
4.81	3.01	0.02	3.34
5.31	2.97	0.02	3.69
5.81	2.94	0.02	4.03
6.31	2.90	0.03	4.38
6.81	2.87	0.04	4.73
7.31	2.84	0.04	5.08
7.81	2.80	0.05	5.42
8.31	2.76	0.05	5.77
8.81	2.74	0.06	6.12
9.31	2.72	0.06	6.47
9.81	2.69	0.07	6.81
10.31	2.66	0.08	7.16
10.81	2.63	0.08	7.51
11.31	2.60	0.09	7.85
11.81	2.57	0.10	8.20
12.31	2.54	0.11	8.55
12.81	2.52	0.11	8.90
13.31	2.49	0.12	9.24
13.81	2.46	0.13	9.59
14.31	2.44	0.13	9.94
14.81	2.42	0.14	10.29
15.31	2.39	0.15	10.63
15.81	2.37	0.16	10.98
16.31	2.35	0.16	11.33
16.81	2.33	0.17	11.68
17.31	2.31	0.18	12.02
17.81	2.27	0.18	12.37
18.31	2.26	0.19	12.72
18.81	2.24	0.20	13.07
19.31	2.22	0.20	13.41
19.81	2.19	0.21	13.76
20.31	2.17	0.22	14.11
20.81	2.15	0.22	14.45
21.31	2.12	0.23	14.80
21.81	2.10	0.24	15.15

22.31	2.07	0.25	15.50
22.81	2.04	0.25	15.84
23.31	2.01	0.26	16.19
23.81	1.98	0.27	16.54
24.31	1.95	0.28	16.89
24.81	1.91	0.29	17.23
25.31	1.89	0.30	17.58
25.81	1.86	0.31	17.93
26.31	1.84	0.32	18.28
26.81	1.81	0.33	18.62
27.31	1.79	0.34	18.97
27.81	1.76	0.34	19.32
28.31	1.74	0.35	19.67
28.81	1.72	0.36	20.01
29.31	1.69	0.37	20.36
29.81	1.66	0.38	20.71
30.31	1.63	0.39	21.05
30.81	1.61	0.41	21.40
31.31	1.58	0.41	21.75
31.81	1.56	0.43	22.10
32.31	1.53	0.44	22.44
32.81	1.50	0.44	22.79
33.31	1.46	0.46	23.14
33.81	1.43	0.46	23.49
34.31	1.40	0.48	23.83
34.81	1.36	0.48	24.18
35.31	1.32	0.50	24.53
35.81	1.27	0.51	24.88
36.31	1.22	0.52	25.22
36.81	1.17	0.53	25.57
37.31	1.13	0.54	25.92
37.81	1.07	0.55	26.26
38.31	1.01	0.56	26.61
38.81	0.96	0.58	26.96
39.31	0.97	0.59	27.31
39.81	0.98	0.60	27.65
40.31	0.96	0.61	28.00
40.81	0.94	0.63	28.35
41.31	0.91	0.64	28.70
41.81	0.87	0.65	29.04
42.31	0.83	0.66	29.39
42.81	0.76	0.68	29.74
43.31	0.68	0.69	30.09

43.81	0.59	0.70	30.43
44.31	0.51	0.71	30.78
44.81	0.42	0.73	31.13
45.31	0.29	0.74	31.48
45.81	0.14	0.75	31.82

Table 4. Energetical efficiency (%) over time.

Time [s]	Voltage [V]	Current [A]	V_H2_exper (cm3)	efficiency of energetical
0.31	3.41	0.00	0.21	0.00
0.81	3.42	0.00	0.56	0.08
1.31	3.42	0.00	0.91	0.00
1.81	3.42	0.00	1.25	0.08
2.31	3.43	0.00	1.60	0.08
2.81	3.43	0.00	1.95	0.08
3.31	3.28	0.01	2.30	0.24
3.81	3.15	0.01	2.64	0.39
4.31	3.06	0.01	2.99	0.53
4.81	3.01	0.02	3.34	0.67
5.31	2.97	0.02	3.69	0.80
5.81	2.94	0.02	4.03	0.94
6.31	2.90	0.03	4.38	1.14
6.81	2.87	0.04	4.73	1.34
7.31	2.84	0.04	5.08	1.54
7.81	2.80	0.05	5.42	1.79
8.31	2.76	0.05	5.77	1.90
8.81	2.74	0.06	6.12	2.09
9.31	2.72	0.06	6.47	2.27
9.81	2.69	0.07	6.81	2.44
10.31	2.66	0.08	7.16	2.68
10.81	2.63	0.08	7.51	2.85
11.31	2.60	0.09	7.85	3.07
11.81	2.57	0.10	8.20	3.29
12.31	2.54	0.11	8.55	3.56
12.81	2.52	0.11	8.90	3.77
13.31	2.49	0.12	9.24	3.97
13.81	2.46	0.13	9.59	4.18
14.31	2.44	0.13	9.94	4.37
14.81	2.42	0.14	10.29	4.57
15.31	2.39	0.15	10.63	4.76

15.81	2.37	0.16	10.98	4.94
16.31	2.35	0.16	11.33	5.07
16.81	2.33	0.17	11.68	5.26
17.31	2.31	0.18	12.02	5.38
17.81	2.27	0.18	12.37	5.53
18.31	2.26	0.19	12.72	5.71
18.81	2.24	0.20	13.07	5.82
19.31	2.22	0.20	13.41	5.93
19.81	2.19	0.21	13.76	6.09
20.31	2.17	0.22	14.11	6.23
20.81	2.15	0.22	14.45	6.38
21.31	2.12	0.23	14.80	6.46
21.81	2.10	0.24	15.15	6.65
22.31	2.07	0.25	15.50	6.76
22.81	2.04	0.25	15.84	6.88
23.31	2.01	0.26	16.19	6.98
23.81	1.98	0.27	16.54	7.17
24.31	1.95	0.28	16.89	7.33
24.81	1.91	0.29	17.23	7.38
25.31	1.89	0.30	17.58	7.55
25.81	1.86	0.31	17.93	7.64
26.31	1.84	0.32	18.28	7.76
26.81	1.81	0.33	18.62	7.89
27.31	1.79	0.34	18.97	7.98
27.81	1.76	0.34	19.32	8.10
28.31	1.74	0.35	19.67	8.16
28.81	1.72	0.36	20.01	8.33
29.31	1.69	0.37	20.36	8.41
29.81	1.66	0.38	20.71	8.50
30.31	1.63	0.39	21.05	8.60
30.81	1.61	0.41	21.40	8.70
31.31	1.58	0.41	21.75	8.76
31.81	1.56	0.43	22.10	8.85
32.31	1.53	0.44	22.44	8.86
32.81	1.50	0.44	22.79	8.85
33.31	1.46	0.46	23.14	8.88
33.81	1.43	0.46	23.49	8.87
34.31	1.40	0.48	23.83	8.86
34.81	1.36	0.48	24.18	8.77
35.31	1.32	0.50	24.53	8.70
35.81	1.27	0.51	24.88	8.58
36.31	1.22	0.52	25.22	8.43
36.81	1.17	0.53	25.57	8.27

37.31	1.13	0.54	25.92	8.10
37.81	1.07	0.55	26.26	7.86
38.31	1.01	0.56	26.61	7.61
38.81	0.96	0.58	26.96	7.42
39.31	0.97	0.59	27.31	7.60
39.81	0.98	0.60	27.65	7.83
40.31	0.96	0.61	28.00	7.82
40.81	0.94	0.63	28.35	7.85
41.31	0.91	0.64	28.70	7.73
41.81	0.87	0.65	29.04	7.54
42.31	0.83	0.66	29.39	7.35
42.81	0.76	0.68	29.74	6.82
43.31	0.68	0.69	30.09	6.21
43.81	0.59	0.70	30.43	5.52
44.31	0.51	0.71	30.78	4.85
44.81	0.42	0.73	31.13	4.03
45.31	0.29	0.74	31.48	2.84
45.81	0.14	0.75	31.82	1.40

3.3.3   Discussion of results

3.3.3.1   Faraday efficiency

Faraday's efficiency defines the fraction between the generated quantity of hydrogen (H_2) and the theoretical hydrogen quantity which could be produced according to the electrical energy input. To calculate the Faraday efficiency, the calculated/theoretical hydrogen volume is first calculated, as the formula [13]:

$$V_{H_2 cal} = \frac{R.I.T.t}{F.p.z} \ (m^3)$$

Where R: gas constat $J/mol.K$, I: current (A), T: tempearature (K), t: time (s), F: Faraday constant (C/mol), p: pressure (Pa), z: number of electrons, N: number cells in the FC system. The gas constant has value $8{,}314 \ \frac{J}{mol.K}$, the experiment is processed inside the lab with room temperature, so $T = 298 \ K$. The value of Faraday constant is given as $F = 96485 \frac{C}{mol}$. The pressure is equal to the atmosphere pressure, $p = 1{,}1013.10^5 \ Pa$. The reactions inside the hydrogen relates to 2 electrons, so $N = 2$ in this experiment. Using formula of theoretical hydrogen, the table 2 is built. The V_{H_2} exper is calculated using the linear formula

$$y = at$$

Where y: the instant V_{H_2} exper, a: the slope of the linear graph in Figure 13, and t: time (s). After the calculation, the Faraday efficiency [13] can be computed as:

$$\gamma_{Far} = \frac{V_{H_2} theor}{V_{H_2} exper} \times 100 \ (\%)$$

As shown in Table 3 and Figure 14, the Faraday efficiency increases over time and remains below 60% in efficiency. This trend indicates that the fuel cell operates at higher power output as the current transitions from the activation loss region to the mass transport region. The observed relationship highlights that the energy required to initiate the reaction in the PEM is the most significant, contributing to the lower efficiency at lower power outputs. As the fuel cell reaches higher power levels, the system becomes more efficient, though it still operates below its theoretical maximum.
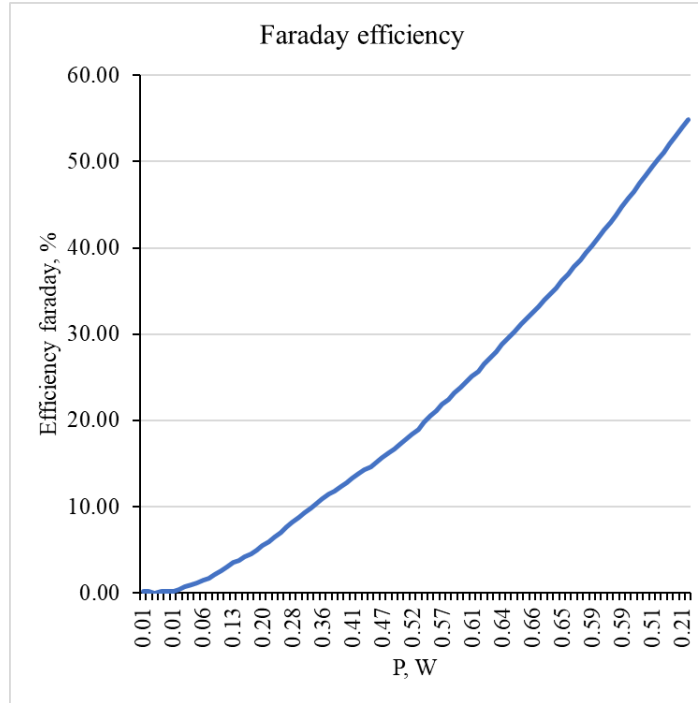

Figure 14. Faraday efficiency (%) of 2nd record in experiment 1.

3.3.3.2 Energetic efficiency

The energy efficiency can be computed as formula [14]:

$$\gamma_{en} = \frac{V.I.t}{V_{H_2exper}.H_v} \times 100 \ (\%)$$

Where, V: voltage (V), I: current (A), t: time (s), $V_{H_2}exper$: expermential H_2 volume (m^3), and H_V: lower heating value of Hydrogen (J/m^3).

The energy efficiency is computed by fraction between the total energy and the expected energy per unit Hydrogen volume, the result is plotted in Figure 15 and calculated in Table 4. Initially, the energy efficiency increases steadily with power, peaking at approximately 8-9% efficiency at around 0.65W, which its voltage around 1.45V and 2,5V. Beyond this operating point, the efficiency begins to decline as the power output increases further. This behavior suggests that the fuel cell operates most efficiently within a specific power range, which aligns with the ohmic region of the fuel cell's characteristic curve. At higher power outputs, the onset of

mass transport limitations and other inefficiencies, such as reactant depletion or water management issues, likely contribute to the observed decrease in efficiency.
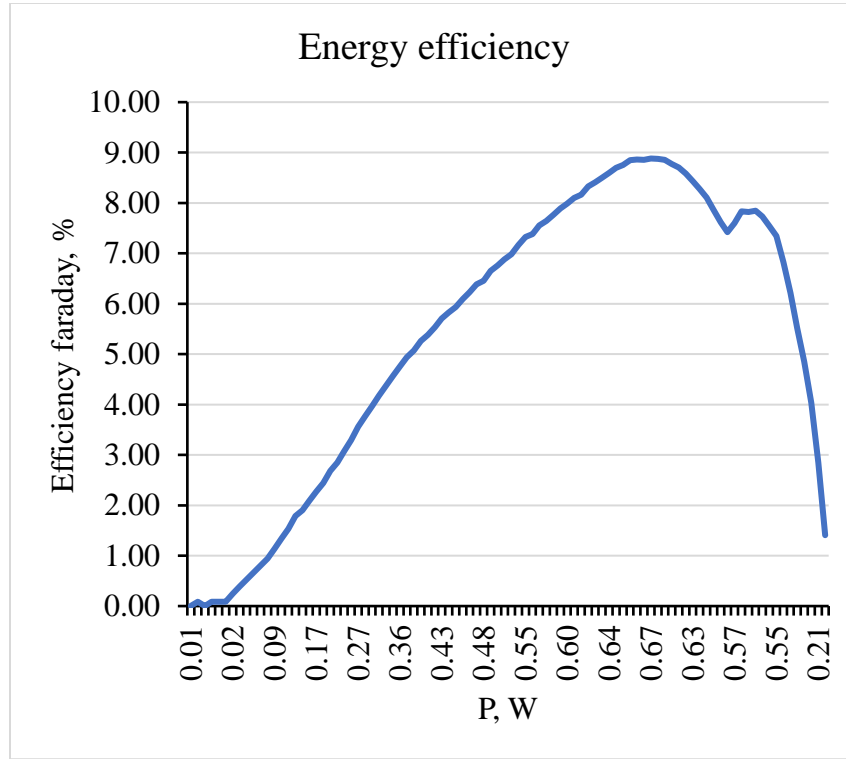

Figure 15. Energy efficiency (%) of 2nd record in experiment 1.

3.3.3.3 Compare between Faraday efficiency and Energy efficiency

The Faraday efficiency is greater than the energy efficiency. This different is since, Faraday efficiency only take account in the losses due to the gas crossover. On the other hand, energy efficiency takes into consideration additional losses such as ohmic losses and joule losses both at the anode and cathode [11].

4   Summary and Outlook

Throughout all three experiments, a deeper understanding of the working principles and performance of the fuel cell system was achieved. The first experiment demonstrated the relationship between voltage, current, and power through the fuel cell's characteristic curve, highlighting the three primary regions: activation losses, ohmic losses, and mass transport losses. A unique phenomenon was also observed, where the accumulation of by-products blocked gas flow, impacting performance. The second experiment provided insights into the fuel cell's behavior when operating at constant voltage across various values and regions, showing that the fuel cell performs most efficiently and maintains balanced power output near its optimal operating point. The final experiment explored the Faraday and energy efficiencies of the fuel cell, revealing that Faraday efficiency is significantly higher than energy efficiency. This is

because Faraday efficiency accounts primarily for gas crossover losses, while energy efficiency includes additional losses such as ohmic and Joule losses.

5 References

1. Karsten, P. (2024) *Electrochemical storage system. Electrochemical storage system*, Karlsruhe: Hochschule Karlsruhe, 7 October.
2. Aminudin, M.A. et al. (2023) 'An overview: Current progress on hydrogen fuel cell vehicles', International Journal of Hydrogen Energy, 48(11), pp. 4371–4388. doi:10.1016/j.ijhydene.2022.10.156.
3. (No date) *Fuel Cell Basics | Department of Energy*. Available at: https://www.energy.gov/eere/fuelcells/fuel-cell-basics (Accessed: 09 November 2024).
4. Hydrogen Fuel News (2024) Why are hydrogen fuel cells so expensive?, Hydrogen Fuel News. Available at: https://www.hydrogenfuelnews.com/hydrogen-fuel-cells-so-expensive/8562913/ (Accessed: 09 November 2024).
5. Fuel cell bipolar plates (no date) Hyfindr.com - the B2B Marketplace for Fuel Cell Components, Hydrogen System and Services. Available at: https://hyfindr.com/en/hydrogen-knowledge/fuel-cell-bipolar-plates (Accessed: 09 November 2024).
6. Tellez-Cruz, M.M. et al. (2021) 'Proton exchange membrane fuel cells (pemfcs): Advances and challenges', Polymers, 13(18), p. 3064. doi:10.3390/polym13183064.
7. (No date a) Hydrogen and Fuel Cell Technology Basics | Department of Energy. Available at: https://www.energy.gov/eere/fuelcells/hydrogen-and-fuel-cell-technology-basics (Accessed: 09 November 2024).
8. U.S. Energy Information Administration - EIA - independent statistics and analysis (no date) Production of hydrogen - U.S. Energy Information Administration (EIA). Available at: https://www.eia.gov/energyexplained/hydrogen/production-of-hydrogen.php#:~:text=Hydrogen%20can%20be%20produced%20from,hydrogen%20production%20methods%2C%20or%20pathways (Accessed: 09 November 2024).
9. (No date a) *Hydrogen Production Processes | Department of Energy*. Available at: https://www.energy.gov/eere/fuelcells/hydrogen-production-processes (Accessed: 09 November 2024).
10. (No date a) *Hydrogen storage | Department of Energy*. Available at: https://www.energy.gov/eere/fuelcells/hydrogen-storage (Accessed: 09 November 2024).
11. Yodwong, B. *et al.* (2020) 'Faraday's efficiency modeling of a proton exchange membrane electrolyzer based on experimental data', *Energies*, 13(18), p. 4792. doi:10.3390/en13184792.
12. LARMINIE, J. (2018) Fuel Cell Systems explained. JOHN WILEY.
13. Faizan, A. (2018) *Fuel cell: Characteristics curve & losses*, *Electrical A2Z*. Available at: https://electricala2z.com/renewable-energy/fuel-cell-characteristics-curve-losses/ (Accessed: 09 November 2024).

14. Karsten, P. (2024) Project A: Fuel Cell, Project - Fuel Cell - WS 2024 / 2025. Edited by M. Aleksandrova. Available at: https://ilias.h-ka.de/goto.php?target=crs_169710&client_id=HSKA#il_mhead_t_focus (Accessed: 30 October 2024).